JOURNAL OF BACTERIOLOGY, Aug. 2010, p. 4089–4102 Vol. 192, No. 16
0021-9193/10/$12.00 doi:10.1128/JB.00201-10

The Rut Pathway for Pyrimidine Degradation: Novel Chemistry and Toxicity Problems▽†

Kwang-Seo Kim,[1]‡ Jeffrey G. Pelton,[2]§‡ William B. Inwood,[1] Ulla Andersen,[2]¶ Sydney Kustu,[1]‖* and David E. Wemmer[2]‖

Departments of Plant and Microbial Biology[1] and Chemistry,[2] University of California, Berkeley, California 94720

Received 26 February 2010/Accepted 2 April 2010

The Rut pathway is composed of seven proteins, all of which are required by *Escherichia coli* K-12 to grow on uracil as the sole nitrogen source. The RutA and RutB proteins are central: no spontaneous suppressors arise in strains lacking them. RutA works in conjunction with a flavin reductase (RutF or a substitute) to catalyze a novel reaction. It directly cleaves the uracil ring between N-3 and C-4 to yield ureidoacrylate, as established by both nuclear magnetic resonance (NMR) spectroscopy and mass spectrometry. Although ureidoacrylate appears to arise by hydrolysis, the requirements for the reaction and the incorporation of ^{18}O at C-4 from molecular oxygen indicate otherwise. Mass spectrometry revealed the presence of a small amount of product with the mass of ureidoacrylate peracid in reaction mixtures, and we infer that this is the direct product of RutA. *In vitro* RutB cleaves ureidoacrylate hydrolytically to release 2 mol of ammonium, malonic semialdehyde, and carbon dioxide. Presumably the direct products are aminoacrylate and carbamate, both of which hydrolyze spontaneously. Together with bioinformatic predictions and published crystal structures, genetic and physiological studies allow us to predict functions for RutC, -D, and -E. *In vivo* we postulate that RutB hydrolyzes the peracid of ureidoacrylate to yield the peracid of aminoacrylate. We speculate that RutC reduces aminoacrylate peracid to aminoacrylate and RutD increases the rate of spontaneous hydrolysis of aminoacrylate. The function of RutE appears to be the same as that of YdfG, which reduces malonic semialdehyde to 3-hydroxypropionic acid. RutG appears to be a uracil transporter.

The *rut* (pyrimidine *ut*ilization) operon of *Escherichia coli* K-12 contains seven genes (*rutA* to *-G*) (31, 38). A divergently transcribed gene (*rutR*) codes for a regulator. The RutR regulator is now known to control not only pyrimidine degradation but also pyrimidine biosynthesis and perhaps a number of other things (44, 45). In the presence of uracil, RutR repression of the *rut* operon is relieved.

Superimposed on specific regulation of the *rut* operon by RutR is general control by nitrogen regulatory protein C (NtrC), indicating that the function of the Rut pathway is to release nitrogen (31, 59). The *rut* operon was discovered in *E. coli* K-12 as one of the most highly expressed operons under NtrC control. *In vivo* it yields 2 mol of utilizable nitrogen per mol of uracil or thymine and 1 mol of 3-hydroxypropionic acid or 2-methyl 3-hydroxypropionic acid, respectively, as a waste product (Fig. 1). Waste products are excreted into the medium. (Lactic acid is 2-hydroxypropionic acid.) Wild-type *E. coli* K-12 can use uridine as the sole nitrogen source at temperatures up to 22°C but not higher. It is chemotactic to pyrimidine bases by means of the methyl-accepting chemoreceptor TAP (taxis toward dipeptides), but this response is not temperature dependent (30).

In the known reductive and oxidative pathways for degradation of the pyrimidine ring (22, 48, 52), the C-5–C-6 double bond is first altered to decrease the aromatic character of the ring, and it is then hydrolyzed between N-3 and C-4 (Fig. 1). We here show that in the Rut pathway the ring is immediately cleaved between N-3 and C-4 by the RutA protein without prior manipulation and hence that RutA is an unusual oxygenase of a type not previously described. We determine the products of the RutB reaction and show that RutA/F and RutB are sufficient to release both moles of ammonium from the pyrimidine ring *in vitro*. Together with the known short-chain dehydrogenase YdfG (18), they yield all of the Rut products obtained *in vivo*.

We use a variety of approaches other than biochemical assays to explore the functions of RutC, -D, and -E. Although these proteins are not required *in vitro*, they are required *in vivo* for growth on uridine as the sole nitrogen source and appear to accelerate removal of toxic intermediates in the Rut pathway or their by-products. We present genetic and physiological evidence that the toxicity of the last Rut intermediate, malonic semialdehyde, rather than the rate of release of ammonium, limits growth on pyrimidines as the sole nitrogen source at high temperatures.

MATERIALS AND METHODS

Bacterial strains. The three strain backgrounds we worked in were wild type (NCM3722), *ntrB*(Con) (*ntrB* [constitutive]; NCM3876), and UpBCon1 (NCM4384). Strains carrying in-frame deletions in each *rut* gene and *ydfG* were constructed in each background by first introducing the appropriate kanamycin

* Corresponding author. Mailing address: Department of Plant & Microbial Biology, University of California, Berkeley, 111 Koshland Hall, Berkeley, CA 94720-3102. Phone: (510) 643-9308. Fax: (510) 642-4995. E-mail: kustu@berkeley.edu.

§ Present address: QB3 Institute, University of California at Berkeley, Berkeley, CA 94720.

¶ Present address: QB3/Chemistry Mass Spectrometry Facility, University of California, Berkeley, CA 94720.

‡ These authors contributed equally to this work.

‖ These authors contributed equally to this work.

† Supplemental material for this article may be found at http://jb.asm.org/.

▽ Published ahead of print on 16 April 2010.

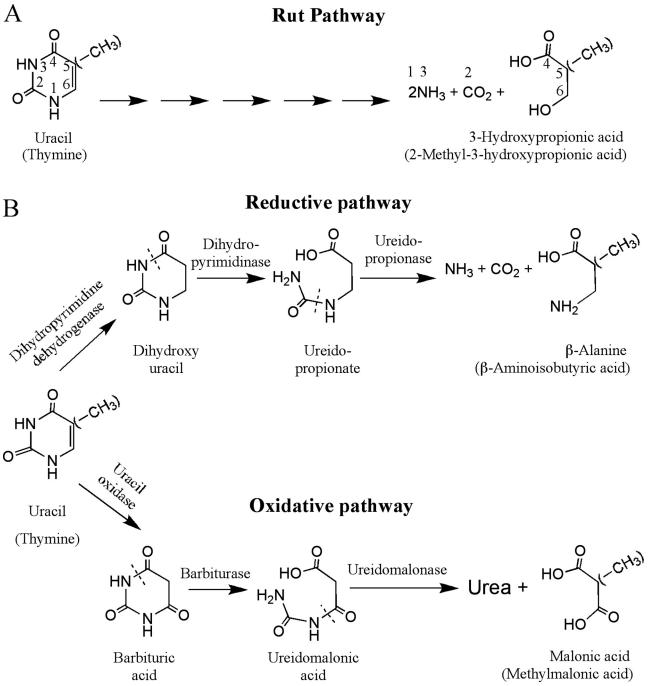

FIG. 1. Comparison of Rut pathway products (*E. coli* K-12) to those of other pyrimidine catabolic pathways. (A) The Rut pathway, which has been studied only *in vivo* in *E. coli* K-12 (31); (B) known reductive (52) and oxidative (22, 28, 48) pathways for catabolism of pyrimidine rings (upper and lower pathways, respectively). Although the enzyme that initiates the oxidative pathway was originally called uracil oxidase, it is a classical monooxygenase (28). An additional pathway (not shown) has recently been proposed in *Saccharomyces kluyveri* (1).

(Kan) insertion by bacteriophage P1-mediated transduction and then deleting it by site-specific recombination (11) (Table 1). The correctness of all deletions was confirmed by sequencing. Due to the absence of four bases in the forward primer for *rutD* (4), RutC extends an additional 36 amino acids in the initial *rutD* deletion strains (Table 1). We do not know how this affects RutC activity. The inadvertent change to RutC was corrected by cloning the *rutC rutD*::Kan fragment from NCM4075 (derived by P1-mediated transduction from NCM4053; Table 1) into the pGEM-T Easy vector and correcting the sequence of the forward primer by site-directed mutagenesis (from ATATCGCAAGTGGGCG CGAGATTCCGGGATC [incorrect] to ATATCGCGAAGTGAGGCCGCGA TGATTCCGGGATC [correct]). After the change to *rutC* was corrected, *rutD*::Kan was introduced into a Δ*rutC* strain (Table 1) (11) and used to generate correct *rutD* deletions in different backgrounds. The *rutF* deletion extended an additional 12 bp beyond its predicted C-terminal end but remained in-frame and within *rutF*. Since *ydfG* is the only gene in its operon, it was not necessary to delete it unless kanamycin sensitivity was required.

Identifications of mutations in strains NCM4139, NCM4299, NCM4300, and NCM4384. An 11-kbp deletion beginning in the *mioC* gene was first found in strain NCM4384 based on tiling microarray data from Roche Nimblegen (23). The extent of the deletion was verified by PCR amplification and sequencing, and the same deletion was found to have occurred independently when a *rutE*::Kan mutation was introduced into the *ntrB*(Con) background by phage P1-mediated transduction (Table 1). Roche 454 deep sequencing (20- to 30-fold coverage) allowed us to identify the remaining mutations. Using *E. coli* K-12 strain MG1655 as a reference strain for the assembly of each of the four genomes, Roche provided tables of differences between each strain and MG1655. These tables were used as a starting point to find mutational changes. By manual inspection of raw sequence data, sequence differences between strains, and contig breaks, we found independent single-base-pair changes associated with *nemR* in strains NCM4139, NCM4299, and NCM4300 and *sroG* in strain NCM4384 (see Results). We then identified the IS*186* insert in the *lon* promoter in strains NCM4139 and NCM4384 by looking for new occurrences of the small insertion elements (IS*1*, IS*2*, IS*3*, IS*4*, IS*5*, IS*30*, IS*150*, and IS*186*).

Growth and toxicity studies. Growth studies were done in N^- C^- minimal medium containing uridine or thymidine as the sole nitrogen source with 0.4% glycerol as the carbon source (31). Studies on solid medium were done with 5 mM uridine or thymidine, as were standard studies on liquid medium. Unless stated otherwise, they were done at room temperature (≤22°C). To measure toxicity, uridine or thymidine (5 mM) was added to ammonium (5 mM) as a nitrogen source and growth was monitored at 37°C.

Cell extracts of UpBCon1 (NCM4384). Cells were grown on minimal medium with glycerol (0.5%) as a carbon source and uridine (5 mM) as the sole nitrogen source at 37°C. They were harvested, washed in 20 mM potassium phosphate buffer (pH 7), and frozen at −80°C. Cells (~0.1 g wet weight/ml) were suspended in potassium phosphate buffer (pH 7) and were disrupted in a French pressure cell (SLM Aminco Instruments, Inc., Rochester, NY) at 6,000 lb/in^2.

Partial purification of His-tagged proteins. ASKA strains JW0997, JW5138, and JW1532, which overproduce His-tagged RutA, RutF, and YdfG protein, respectively (26), were grown on Luria broth containing chloramphenicol (25 μg/ml) to an optical density at 600 nm (OD_{600}) of ~0.5, and expression was induced for 3 to 4 h by addition of IPTG (isopropyl-β-D-thiogalactopyranoside) (to 100 μM). Cells were harvested and frozen at −80°C until use. They were suspended at ~0.1 g wet weight/ml in 20 mM phosphate buffer (pH 7) and were disrupted as described above. His-tagged RutA protein was then partially purified using Ni^+-nitrilotriacetic acid (NTA) agarose (Qiagen, Valencia, CA) according to the manufacturer's instructions and was finally dialyzed four times against 500 ml of 20 mM phosphate buffer (pH 7) at 4°C and stored in small aliquots at −80°C (see Fig. S1 in the supplemental material). The RutF protein was not well overexpressed and was assayed only in extracts. Protein concentrations were determined using the Micro bicinchoninic acid (BCA) protein assay kit (Thermo Scientific, IL). The Fre flavin reductase, a kind gift from Luying Xun, Washington State University, Pullman, was purified as described previously (58) and was stored at −80°C. Before use, it was diluted in 20 mM phosphate buffer (pH 7) containing 1 mM dithiothreitol (DTT). The RutB protein was used from extracts of JW5139. His-tagged RutB protein was a kind gift from Tathagata Mukherjee and Tadhg Begley, Cornell University and Texas A and M University, respectively.

Materials for the RutA/F reaction. [^{14}C-2]- and [^{14}C-6]uracil were purchased from MP Biomedicals (Solon, OH). [^{14}C-methyl]thymine was purchased from Moravek Biochemicals and Radiochemicals (Brea, CA). Uniformly labeled [^{13}C, ^{15}N]uracil (99%, 98%), [^{15}N]uracil (98%), [^{13}C-4, ^{13}C-5]uracil (99%), and $^{18}O_2$ (97%) were purchased from Cambridge Isotope Laboratories, Inc. (Andover, MA).

Assay for the RutA protein. Reaction mixtures contained 40 mM Tris buffer (pH 8.2) or 40 mM phosphate buffer (pH 7), 20 μM flavin mononucleotide (FMN), 4 mM NADH, and 0.4 mM uracil. For standard reactions, we used 18 μg of His_6-RutA, 6 μg of Fre, and [^{14}C]uracil (radiolabeled at position 2 or 6 at 2×10^7 cpm) in a total volume of 120 μl. Reaction mixtures were incubated at room temperature with agitation for 20 min, and reactions were stopped by putting them on ice and then freezing them at −20°C. Products were analyzed on cellulose F thin-layer chromatography (TLC) plates (Merck, Germany) in developing solution containing isopropyl alcohol-water (3:1).

For $^{18}O_2$ labeling of the RutA product, the total volume of reaction mixtures was increased 5-fold. All components except enzymes were mixed, and reaction mixtures were bubbled with N_2 for 5 min. They were then bubbled with $^{18}O_2$ or $^{16}O_2$ for 1 min. During bubbling with O_2, His_6-RutA and Fre were added and bubbling was continued for an additional 5 min. For analysis of 50:50 mixtures of $^{18}O_2$- and $^{16}O_2$-labeled products, equal volumes of separate reaction mixtures were combined.

Synthesis of *Z*-3-ureido-2-propenoic acid. *Z*-3-Ureido-2-propenoic acid (ureidoacrylate) was synthesized by adding 3 ml of 4 M ammonium hydroxide to 100 mg of 2,3-dihydro-1,3-6H-oxazine-2,6-dione (3-oxauracil) (Research Organics, Inc., Cleveland, OH) on ice as described previously (16). The reaction was allowed to proceed for 12 h at room temperature, after which 1 ml of 1 M NaOH was added, and the solution was lyophilized to dryness. The product was extracted by adding 1 ml of methanol to the dried powder. The product was obtained by lyophilizing the methanol fraction. The presence of the correct product was confirmed by comparing ^{1}H-nuclear magnetic resonance (NMR) chemical shifts and coupling constants in dimethyl sulfoxide (DMSO) with published values (16).

1D ^{13}C NMR spectra. For NMR studies, the RutA reaction was performed using uniformly ^{13}C/^{15}N-labeled uracil (Cambridge Isotope Labs, Andover, MA) as the substrate, unless stated otherwise. Reaction mixtures prepared and frozen as described above were used as such or were lyophilized and dissolved in

TABLE 1. Strains used in this study

Strain	Relevant genotype or description	Construction or reference
NCM3722	*E. coli* K-12 prototroph	49
NCM3876	*glnL2302* [*ntrB*(Con)]	21
NCM4047	Δ*rutG750*::Kan (JW5137)[a]	4
NCM4049	Δ*rutF751*::Kan (JW5138)	4
NCM4051	Δ*rutE752*::Kan (JW0993)	4
NCM4053	Δ*rutD753*::Kan (JW0994)	4
NCM4055	Δ*rutC754*::Kan (JW0995)	4
NCM4057	Δ*rutB755*::Kan (JW5139)	4
NCM4059	Δ*rutA756*::Kan (JW0997)	4
NCM4072	Δ*rutG750*::Kan	P1[b](NCM4047) → NCM3722
NCM4074	Δ*rutE752*::Kan	P1(NCM4051) → NCM3722
NCM4088	Δ*rutD*[c]	P1(NCM4053) → NCM3722, FLP[d]
NCM4090	Δ*rutD ntrB*(Con)	P1(NCM4053) → NCM3876, FLP
NCM4092	Δ*rutB*	P1(NCM4057) → NCM3722, FLP
NCM4094	Δ*rutB ntrB*(Con)	P1(NCM4057) → NCM3876, FLP
NCM4101	Δ*rutF*[e]	P1(NCM4049) → NCM3722, FLP
NCM4103	Δ*rutE*	P1(NCM4051) → NCM3722, FLP
NCM4105	Δ*rutC*	P1(NCM4055) → NCM3722, FLP
NCM4107	Δ*rutA*	P1(NCM4059) → NCM3722, FLP
NCM4111	Δ*rutG ntrB*(Con)	P1(NCM4047) → NCM3876, FLP
NCM4113	Δ*rutF*[e] *ntrB*(Con)	P1(NCM4049) → NCM3876, FLP
NCM4115	Δ*rutE ntrB*(Con)	P1(NCM4051) → NCM3876, FLP
NCM4117	Δ*rutC ntrB*(Con)	P1(NCM4055) → NCM3876, FLP
NCM4119	Δ*rutA ntrB*(Con)	P1(NCM4059) → NCM3876, FLP
NCM4139	*ntrB*(Con) UpBCon2	Spont.[f], growth on uridine at 37°C
NCM4230	Δ*ydfG760*::Kan (JW1532)	4
NCM4299	*ntrB*(Con) Δ*rutE sup1*[g]	Spont., growth on uridine at room temp
NCM4300	*ntrB*(Con) Δ*rutE sup2*	Spont., growth on uridine at room temp
NCM4384	*ntrB*(Con) UpBCon1	Spont., growth on uridine at 37°C
NCM4507	Δ*rutG ntrB*(Con) UpBCon1	P1(NCM4047) → NCM4384, FLP
NCM4508	Δ*rutF ntrB*(Con) UpBCon1	P1(NCM4049) → NCM4384, FLP
NCM4509	Δ*rutE ntrB*(Con) UpBCon1	P1(NCM4051) → NCM4384, FLP
NCM4510	Δ*rutD*[c] *ntrB*(Con) UpBCon1	P1(NCM4053) → NCM4384, FLP
NCM4511	Δ*rutC ntrB*(Con) UpBCon1	P1(NCM4055) → NCM4384, FLP
NCM4512	Δ*rutB ntrB*(Con) UpBCon1	P1(NCM4057) → NCM4384, FLP
NCM4513	Δ*rutA ntrB*(Con) UpBCon1	P1(NCM4059) → NCM4384, FLP
NCM4713	Δ*ydfG760*::Kan	P1(NCM4230) → NCM3722
NCM4714	Δ*ydfG760*::Kan *ntrB*(Con)	P1(NCM4230) → NCM3876
NCM4715	Δ*ydfG760*::Kan *ntrB*(Con) UpBCon1	P1(NCM4230) → NCM4384
NCM4852	Δ*ydhM727*::Kan (JW5874)	4
NCM4853	*rutD*::Kan[h]	Fragment[i] electroporation → NCM4105
NCM4861	Δ*rutD*[h]	NCM4853, FLP
NCM4904	Δ*nemR ntrB*(Con)	P1(NCM4852) → NCM3876, FLP
NCM4905	Δ*rutE* Δ*nemR ntrB*(Con)	P1(NCM4852) → NCM4115, FLP
NCM4906	Δ*rutE ntrB*(Con) UpBCon2	P1(NCM4074) → NCM4139, FLP
NCM4913	Δ*rutD*::Kan[h] *ntrB*(Con)	P1(NCM4853) → NCM3876
NCM4915	Δ*rutD*::Kan[h] *ntrB*(Con) UpBCon1	P1(NCM4853) → NCM4384
NCM4916	Δ*ydfG760*::Kan *ntrB*(Con) UpBCon2	P1(NCM4713) → NCM4139
NCM4918	Δ*rutD*[h] *ntrB*(Con)	NCM4913, FLP
NCM4920	Δ*rutD*[h] *ntrB*(Con) UpBCon1	NCM4915, FLP
NCM4969	Δ*ydfG760*::Kan Δ*nemR ntrB*(Con)	P1(NCM4713) → NCM4904

[a] Strains with JW numbers were obtained directly from the Mori collection in Japan; later changes in their designation upon transfer to the *E. coli* Genetic Stock Center are not indicated here. In addition to the relevant mutation, the genotype of these strains is F$^-$ Δ(*araD-araB*)*567* Δ*lacZ4787*(::*rrnB-3*) λ$^-$ *rph-1* Δ(*rhaD-rhaB*)*568 hsdR514*.

[b] Phage P1-mediated transduction.

[c] The sequence for RutC extends an additional 36 amino acids in the *rutD* gene due to the absence of four bases in the forward primer designed for *rutD* (4). We do not know how this affects RutC activity. The strain also carries a suppressor mutation.

[d] Insertion removed by site-specific recombination using the FLP recombinase (4, 11).

[e] The *rutF* deletion extended an additional 12 bp beyond its predicted C-terminal end but remained in-frame and within *rutF*.

[f] Spont., spontaneous (see the text).

[g] sup, suppressor.

[h] RutC is normal.

[i] The fragment carried *rutC*$^+$ *rutD*::Kan (see Materials and Methods).

DMSO. One-dimensional (1D) ^{13}C spectra were recorded on a Bruker Avance 600-MHz spectrometer equipped with a CPTXI cryoprobe in 4 to 16 h and a Bruker Avance 800-MHz spectrometer equipped with a TXI probe in 24 to 48 h. In all cases, ^{1}H decoupling was applied during acquisition, and data were zero-filled once before analysis. Spectra recorded in H_2O were referenced to 4,4-dimethyl-4-silapentane-1 sulfonic acid (DSS; 0 ppm), and samples dissolved in DMSO were referenced to tetramethylsilane (TMS; which replaces the DMSO resonance at 39.5 ppm). For complete ^{13}C spectra of the product, the carrier and

spectral width were set to 127 ppm and 130 ppm, respectively, and the final digital resolution was approximately 6 Hz/point. For identification of ^{16}O-to-^{18}O isotope shifts, RutA reactions were performed with either $^{16}O_2$ or $^{18}O_2$ (Cambridge Isotope Labs, Andover, MA) and [^{13}C-4, C-5]uracil (Cambridge Isotope Labs, Andover, MA); equal amounts of the two reaction mixtures were combined. Spectra were taken in DMSO, and data were recorded at 800 MHz. The ^{13}C carrier frequency and spectral width were set to 164 ppm and 25 ppm, respectively. The final digital resolution was 1.2 Hz/point.

2D NMR spectra. A 2D ^1H-^{13}C heteronuclear single quantum coherence (HSQC) spectrum (43) of the product was recorded at 800 MHz in D_2O by lyophilizing the sample from H_2O and redissolving it in 100% D_2O. A total of 1,024 and 512 points were collected in the ^1H and ^{13}C dimensions, respectively. The carrier frequencies were set to 5.2 ppm (^1H) and 118 ppm (^{13}C), and the spectral widths were set to 13 ppm (^1H) and 80 ppm (^{13}C). The spectrum was recorded in 18 h and was processed with NMRPipe software (12). After zero-filling twice in the ^{13}C dimension, the digital resolution was 16 Hz/point. Chemical shifts were indirectly referenced to DSS (57).

The number of protons attached to the product N-3 resonance was determined by examining the ^1H-^{15}N coupling pattern in a 2D ^{13}C-detected ^{15}N-^{13}C HSQC experiment (6) on the reaction mixture in H_2O. The spectrum was recorded on an Avance II 900-MHz instrument equipped with a CPTXI cryoprobe using the C_CO_N HSQC pulse sequence supplied by Bruker-Biospin, Inc. However, no ^1H decoupling was applied in the ^{15}N dimension, and no ^{15}N decoupling was applied during detection of ^{13}C. Totals of 8,192 points and 120 points were collected in the ^{13}C and ^{15}N dimensions, respectively. The carrier frequencies were set to 170 ppm (^{13}C) and 95 ppm (^{15}N), and spectral widths were set to 80 ppm (^{13}C) and 87.5 ppm (^{15}N). The total experiment time was 14 h. The data were processed with NMRPipe software (12). Data in the ^{15}N dimension were increased to 256 points by linear prediction and subsequently to 512 points by zero-filling. The final resolutions were 4.4 Hz and 15.6 Hz in the ^{13}C and ^{15}N dimensions, respectively.

MS. Liquid chromatography-mass spectrometry (LC/MS) data were obtained using an Agilent 1200 liquid chromatograph coupled to an LTQ Orbitrap mass spectrometer. The Orbitrap mass spectrometer was operated in positive-mode electrospray ionization with a mass resolution of 30,000. A Phenomenex Capcell C_{18} column (5μ, 120 Å, 150 by 4.6 mm) with a flow rate of 0.2 ml/min was used for optimum chromatographic separation. For the ureidoacrylate compounds, an isocratic gradient of 10% acetonitrile, 89% water, and 1% formic acid was used. For the peroxy form, a gradient of 0 to 50% methanol over 20 min was used.

Assay for the RutB protein. The RutB protein was assayed using ^{14}C-labeled RutA product as the substrate and monitoring by TLC as described above or using chemically synthesized ureidoacrylate (16) and monitoring the decrease in absorbance at 266 nm with extinction coefficients of 17,800 M^{-} Cm^{-} in 0.025 M HCl (16) and 18,300 in 40 mM Tris buffer (pH 8.2). Formation of ammonia was monitored by coupling to the glutamate dehydrogenase reaction and measuring NADPH oxidation (ammonia assay kit; Sigma, St. Louis, MO). Formation of malonic semialdehyde was assayed by coupling to YdfG (18). Reaction mixtures contained 40 mM Tris (pH 8.2), 0.25 mM ureidoacrylate, 0.8 mM NADPH, 28 μg of RutB, and 4.5 μg of YdfG in a total volume of 400 μl. They were incubated at room temperature for 3 h. Consumption of ureidoacrylate and of NADPH was determined using their extinction coefficients, ammonium was determined as described above, and 3-hydroxypropionic acid was identified and quantified by GC/MS as described previously (31). We verified that YdfG oxidized serine and 3-hydroxypropionic acid as described previously (18). Reaction mixtures contained 200 mM Tris (pH 8.5), 1 mM NADP, 12 μg YdfG, and 0.5 M L-serine or 3-hydroxypropionic acid in a total volume of 400 μl. NADPH formation was monitored at 340 nm at room temperature. The 3-hydoxypropionic acid (NH_4^+ salt; 138 mg/ml) was kindly provided by Hans Liao (Cargill Corporation, Minneapolis, MN).

RESULTS

Isolation of strains that utilize pyrimidines as the sole nitrogen source at 37°C. In a wild-type *E. coli* K-12 strain, the *rut* operon allows growth on pyrimidines as the sole nitrogen source at temperatures up to ~22°C but not higher (31). Expression of the operon is elevated in a strain that carries an *ntrB*(Con) (*ntrB* [constitutive]) mutation, which increases transcription of all genes under NtrC control (59). In an *ntrB*(Con) background (NCM3876), we isolated two strains that could grow on uridine at 37°C, UpBCon1 (NCM4384) and UpBCon2 (NCM4139). The former, which grew fastest, excreted a yellow compound into the medium and grew poorly at room temperature even on enriched medium. At 37°C, it obtained both nitrogens from uridine in usable form and excreted 1 mol/mol of 3-hydroxypropionic acid into the medium (see Table S1 in the supplemental material) (31).

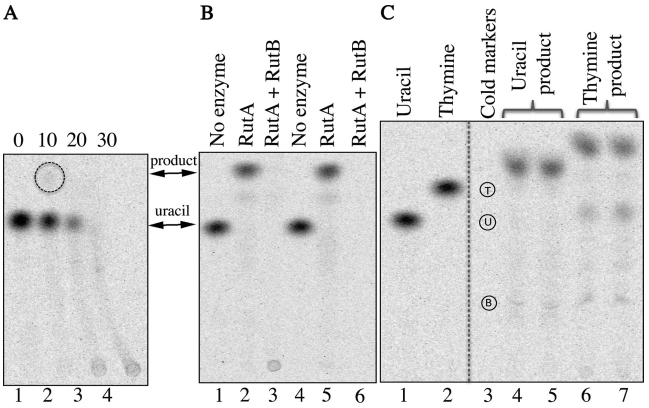

FIG. 2. RutA acts on [^{14}C]uracil and thymine. (A) Products from [^{14}C-6]uracil in the presence of increasing amounts of cell extract (μl) from NCM4384 (UpBCon1) grown on uridine at 37°C. (B) Products from [^{14}C-6]uracil (lanes 1 to 3) or [^{14}C-2]uracil (lanes 4 to 6) in the presence of RutA (lanes 2 and 5) or RutA and RutB (lanes 3 and 6). Samples in lanes 1 and 4 are from controls with no enzyme. (C) Products from [^{14}C-6]uracil (lanes 4 and 5) or [$^{14}CH_3$]thymine (lanes 6 and 7) in the presence of RutA. Samples in lanes 1 and 2 are from controls with no enzyme, and the sample in lane 3 contained a mixture of unlabeled thymine (T), uracil (U), and barbituric acid (B), which were detected by UV absorbance and have been circled. All reactions mixtures that contained RutA also contained the flavin reductase Fre. Reactions were run for 20 min at room temperature with agitation as described in Materials and Methods, and the mixtures were frozen at −20°C before being analyzed by thin-layer chromatography. For samples in panels A and C, reactions were run at pH 8.2, and for samples in panel B, they were run at pH 7.

Degradation of ^{14}C-labeled uracil or thymine by cell extracts. To initiate studies of Rut enzymes *in vitro*, we first prepared cell extracts of NCM4384 (UpBCon1) grown on uridine at 37°C. Bioinformatic predictions were that the RutA protein was a monooxygenase with alkane sulfonate monooxygenase as its closest homologue and that the RutF protein was a flavin reductase with the HpaC protein, which functions in the oxidation of 4-hydroxyphenylacetate in *E. coli* W, as its closest homologue (13, 19, 31). In the presence of cell extract, FMN, and NADH, [^{14}C]uracil labeled at C-6 or C-2 was consumed (Fig. 2A) (data not shown). FAD worked much less well than FMN, and NADPH worked much less well than NADH. HpaC also has a strong preference for FMN and NADH (19). As the amount of extract was increased, only a small amount of label from C-6 of the uracil ring remained on cellulose TLC plates, near the origin (Fig. 2A), and label from C-2 was completely lost.

The RutA/F reaction. His-tagged RutA was well overexpressed from ASKA strain JW0997 and could be purified by Ni^{2+} chelate chromatography (Materials and Methods) (see Fig. S1 in the supplemental material). His-tagged RutF was not well overexpressed, but we were able to use another highly purified flavin reductase, Fre (58), in its place for most of our

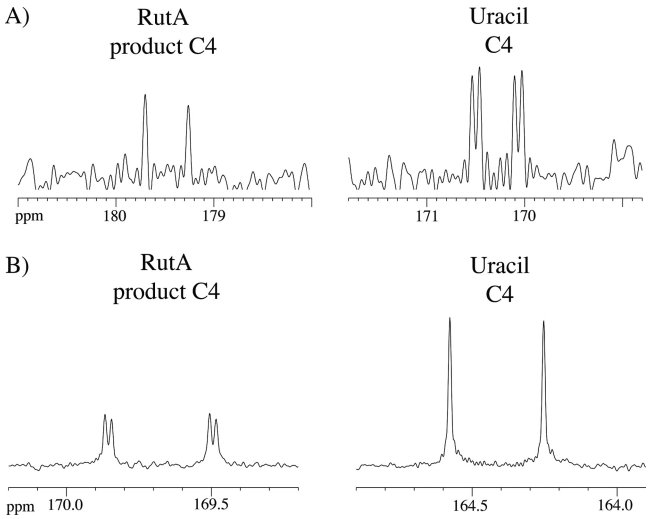

FIG. 3. NMR evidence that RutA cleaves the uracil ring between N-3 and C-4 and incorporates O from O_2 at C-4. (A) 1D ^{13}C-NMR spectrum of the C-4 resonances of the product of the RutA reaction (RutA product C4) and uracil (Uracil C4). Uracil was uniformly ^{13}C/^{15}N labeled. The C-4 resonance of uracil shows a large coupling of 65 Hz to C-5 and a small coupling of 11 Hz to N-3. The C-4 resonance of the product lacks the coupling to N-3, indicating that the bond between N-3 and C-4 was broken. The spectrum was recorded at 600 MHz. (B) The spectrum is as in panel A, except that [^{13}C-4, C-5]uracil was used, the RutA reaction mixtures were bubbled with $^{18}O_2$ or $^{16}O_2$, and then equal volumes were combined. The uracil and product C-4 resonances are split by the $^1J_{C-4–C-5}$ coupling of 65 Hz. The product C-4 resonance also exhibits an ^{18}O isotope shift of −0.02 ppm, indicating that oxygen was incorporated at this position. The spectrum was recorded at 800 MHz. The different chemical shifts of the species in panels A and B result from the fact that spectrum A was recorded in H_2O, whereas spectrum B was recorded in DMSO.

studies. In the presence of both RutA and Fre (or an extract containing RutF) and the necessary flavin and pyridine nucleotide cofactors, [^{14}C]uracil labeled at C-2 or C-6 was converted to a product with faster mobility on TLC plates (Fig. 2B). The product appeared to be more stable at pH 7 than 8.2 (data not shown). Addition of catalase to reaction mixtures to remove any H_2O_2 generated by the flavin reductase did not affect the behavior of the RutA product on TLC plates but did clear the background. [Methyl-^{14}C]thymine was also converted to a product with faster mobility (Fig. 2C).

To identify the product produced from uracil in the RutA/F reaction, we prepared it from ^{13}C- and ^{15}N-enriched uracil. A 2D NMR ^{1}H-^{13}C correlation spectrum in D_2O confirmed that a single product was produced (see Fig. S2A in the supplemental material). A 1D carbon spectrum showed that splitting of the ^{13}C-4 signal by ^{15}N-3 was lost in the product, whereas splitting by ^{13}C-5 was retained. This indicated that the uracil ring had been cleaved between N-3 and C-4 (Fig. 3A). We were unable to obtain ^{13}C, ^{15}N-enriched thymine commercially. However, we showed that the product from unlabeled thymine had only one new H-6–H-5 methyl correlation in a 2D ^{1}H total correlation spectroscopy (TOCSY) spectrum, indicating that a single product was produced and that the C-5–C-6 bond was intact (data not shown). The magnitudes of the chemical shift changes for this product were similar to those for the product from uracil, providing evidence that the two products were analogous.

TABLE 2. NMR chemical shifts of the RutA product are identical to those of synthetic ureidoacrylate

Position	Chemical shift (ppm) in H_2O relative to DSS	
	RutA product[a]	Ureidoacrylate[b]
H-5	4.93	4.92
H-6	7.08	7.10
C-2	160.3	160.3
C-4	179.5	179.6
C-5	103.1	103.2
C-6	138.02	138.1

[a] Prepared at pH 7 as described in Materials and Methods.
[b] Chemically synthesized from 3-oxauracil (see Materials and Methods).

To further characterize the product from uracil, we prepared it from ^{13}C-4, C-5-enriched uracil and a 50:50 mixture of $^{18}O_2$ and $^{16}O_2$. An isotope shift in the 1D carbon spectrum indicated that an oxygen atom derived from molecular oxygen was bound to C-4 (Fig. 3B) (16). A ^{1}H-^{15}N correlation spectrum showed that there was no ^{18}O bound to N-3 because the N-3 resonance failed to show the isotope shift of 0.138 ppm that would be expected if ^{18}O were directly bonded to it (data not shown). Moreover, a carbon-nitrogen HSQC spectrum on product labeled with ^{13}C and ^{15}N but not ^{18}O indicated that N-3 had been converted to NH_2 (see Fig. S2B in the supplemental material). All of the findings were in agreement with ureidoacrylate as the product.

To confirm the identity of the RutA/F product, we chemically synthesized ureidoacrylate (*Z*-3-ureido-2-propenoic acid) from 3-oxauracil as described in Materials and Methods. The ^{13}C and ^{1}H shifts for the RutA/F product were the same as those for synthetic ureidoacrylate (Table 2), and the ^{1}H shifts and *J* couplings of the synthetic compound agreed well with published values (Table 3).

Finally, we obtained mass spectral data on the RutA/F product prepared from $^{18}O_2$ and a 50:50 mixture of ^{13}C/^{15}N-labeled and unlabeled uracil. Accurate mass measurements for both the ^{13}C/^{15}N and unlabeled product species were in agreement with the calculated mass values for ureidoacrylate (Fig. 4A and 5A). Mass spectral analysis of the RutA/F product prepared as described above also revealed a weak peak at 157.0567, which matches the theoretical mass of a ^{13}C/^{15}N-labeled species containing two atoms of ^{18}O from molecular oxygen (within 5 ppm; theoretical value, 157.0560). Accurate mass measurements of product prepared from a mixture of ^{13}C/^{15}N-labeled

TABLE 3. NMR chemical shifts and coupling constants[a] of ureidoacrylate are identical to the published values

Position	Chemical shift (ppm) in DMSO relative to TMS	
	Ureidoacrylate[b]	Published value[c]
H-1	9.75	9.76
H-5	4.73	4.79
H-6	7.31	7.32

[a] The measured coupling constants were 9.0 Hz for: $^1J_{5,6}$ (the same as the published value) and 12.0 Hz for $^1J_{1,6}$ (versus the published value of 11.7 Hz).
[b] Chemically synthesized from 3-oxauracil (see Materials and Methods).
[c] See reference 16.

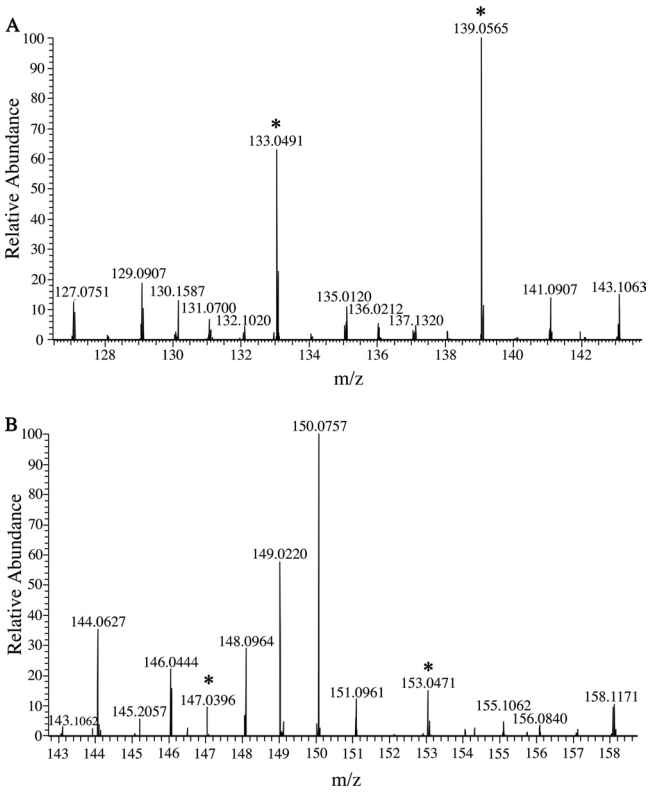

FIG. 4. Mass spectrometric evidence that RutA yields ureidoacrylate and a trace of its peracid. (A) Ureidoacrylate *m/z* 133.0491 corresponds to $[C_4H_6N_2{}^{16}O_2{}^{18}O + H]^+$ (calculated value, 133.0494); *m/z* 139.0565 corresponds to $[^{13}C_4H_6{}^{15}N_2{}^{16}O_2{}^{18}O + H]^+$ (calculated value, 139.0569). (B) Peracid of ureidoacrylate. *m/z* 147.0396 corresponds to $[C_4H_6N_2O_4 + H]^+$ (calculated value, 147.0400); *m/z* 153.0471 corresponds to $[^{13}C_4H_6{}^{15}N_2O_4 + H]^+$ (calculated value, 153.0475).

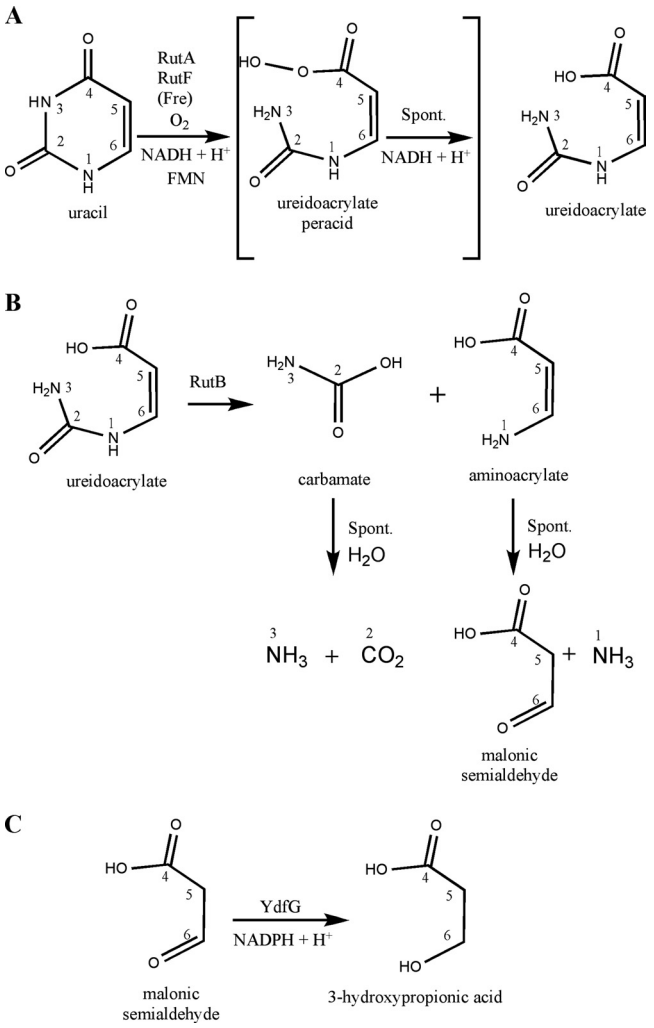

FIG. 5. *In vitro* reactions catalyzed by RutA/F, RutB, and the short-chain dehydrogenase YdfG. (A) RutA/F reaction. The RutA/F reaction yields ureidoacrylate *in vitro*. However, there also appears to be a small amount of ureidoacrylate peracid in reaction mixtures (Fig. 4B), and we infer that this is the product of the RutA/F reaction. Mukherjee et al. (37) have evidence that the peracid is quickly reduced to ureidoacrylate by NADH spontaneously (Spont.) under conditions similar to ours (see Discussion and Fig. 6) (B) RutB reaction. The RutB reaction yields 2 mol of ammonium, HCO_3^-, and malonic semialdehyde (3-oxopropionate) from ureidoacrylate. Carbamate and aminoacrylate, which hydrolyze spontaneously, are the presumed intermediates. (C) YdfG reaction. The known short-chain dehydrogenase YdfG (18) reduces malonic semialdehyde to 3-hydroxypropionic acid. In our case, malonic semialdehyde was generated from ureidoacrylate by the RutB reaction, which was run simultaneously.

and unlabeled uracil but with $^{16}O_2$ confirmed the presence of this species, which appeared to be the peracid of ureidoacrylate (Fig. 4B and 5A). In the latter case, peaks were strong enough that both the $^{13}C/^{15}N$-labeled and unlabeled species containing two atoms of ^{16}O were observed. We return to the significance of this in the Discussion.

The RutB reaction. RutB was initially predicted to be an isochorismatase and later a homologue of *N*-carbamoylsarcosine amidohydrolase (31, 32). To see whether RutB would hydrolyze ureidoacrylate, the product we obtained from the RutA/F reaction, we first used RutA and the substitute flavin reductase Fre to prepare radiolabeled ureidoacrylate from uracil. When [^{14}C]ureidoacrylate was treated with His-tagged RutB, ^{14}C label originating from C-2 of uracil was lost from TLC plates, as was standard [^{14}C]HCO_3^- (data not shown). Label from C-6 smeared near the origin. The same result was obtained if the RutA, Fre, and RutB proteins were added to radiolabeled uracil simultaneously (Fig. 2B, lanes 3 and 6). Likewise, label from uracil was largely lost when cell extracts rather than purified enzymes were added to [^{14}C-2] (data not shown) or [^{14}C-6]uracil (Fig. 2A): at most, traces of RutA/F product were observed. When chemically synthesized ureidoacrylate was used as the substrate for RutB, approximately 2 mol of ammonium was released per mol of uracil consumed (see Fig. S3 in the supplemental material).

Hydrolytic cleavage of ureidoacrylate between N-1 and C-2 would release carbamate and aminoacrylate (Fig. 5B). The carbamate would in turn hydrolyze spontaneously to ammonium and CO_2, thus accounting for production of 1 mol of ammonium and loss of label from C-2 (46, 47). The aminoacrylate would hydrolyze spontaneously to ammonium and malonic semiadehyde, accounting for the second mole of ammonium.

To determine whether the RutB reaction released carbons 4 to 6 of the uracil ring as malonic semialdehyde, we made use of

TABLE 4. Production of 3-OH propionate from ureidoacrylate by RutB and YdfG

Substrate or product and activity	Amt (μM) of substrate or product consumed, produced, or oxidized in:		
	Expt 1[a]	Expt 2[b]	Expt 3[c]
Ureidoacrylate consumed	225		
3-OH propionate produced[d]	210	384	168
NADPH oxidized	173[e]		
NH_4^+ produced[f]	474	918	884

[a] The initial ureidoacrylate concentration was 250 μM. RutB and YdfG were added simultaneously and incubated for 3 h at room temperature.
[b] The initial ureidoacrylate concentration was 450 μM. RutB and YdfG were added simultaneously and incubated for 6 h at room temperature.
[c] The initial ureidoacrylate concentration was 450 μM. RutB was added first. After 3 h at room temperature, YdfG was added for an additional 3 h.
[d] A total of 380 μl of the total 400-μl reaction mixture was used, and 3-OH propionate was measured as described previously (31) using the standard described in Materials and Methods.
[e] In an additional experiment, 226 μM NADPH was oxidized.
[f] Twenty microliters of the total reaction mixture was used.

TABLE 5. Growth of *rut* strains on uridine[a]

Deletion[b]	Background		
	Wild type (NCM3722), growth at room temp	*ntrB*(Con) (NCM3876), growth at room temp	UpBCon1 (NCM4384), growth at 37°C
rutA	−	−	−
rutB	−	−	−
rutC	− (suppressors)	+/−[c]	−
rutD[d]	− (suppressors)	− (suppressors)	ND[f]
rutE	−	− (suppressors)	+/−
rutF[e]	−	− (suppressors)	−
ydfG	+/−	− (suppressors)	+/− (suppressors)

[a] Strains were grown on minimal agar plates with glycerol as the carbon source and 5 mM uridine as the sole nitrogen source (31).
[b] Nonpolar deletions confirmed by sequencing.
[c] +/−, poor growth.
[d] A *rutD* deletion mutant that did not affect RutC was constructed late in the study, as described in Materials and Methods and Table 1.
[e] The *rutF* deletion extended an additional 12 bp beyond its predicted C-terminal end but remained in-frame and within *rutF*.
[f] ND, not determined.

E. coli K-12 YdfG protein, a short-chain dehydrogenase that is known to oxidize 3-hydroxypropionate and inferred to act in the reductive direction *in vivo* (18). (YdfG also oxidizes serine, and its best substrate is L-*allo*-threonine.) When RutB, YdfG, and NADPH were added to chemically synthesized ureidoacrylate simultaneously, approximately 1 mol of 3-hydroxypropionate was produced per mol of ureidoacrylate consumed, indicating that RutB did indeed release malonic semialdehyde (Table 4 and Fig. 5C). One mole of NADPH was oxidized and, as expected, approximately 2 mol of NH_4^+ was released. If the RutB reaction was allowed to proceed first and then YdfG was added later, the yield of NH_4^+ remained the same but the yield of 3-hydroxypropionate was greatly reduced (Table 4), possibly due to the formation of adducts by malonic semialdehyde (17). This might also account for the smearing and loss of malonic semialdehyde from TLC plates.

Requirement for the RutA, -B, and -F proteins *in vivo*. We constructed strains carrying nonpolar deletions in the *rut* genes in three backgrounds: an otherwise wild-type background; the *ntrB*(Con) background, in which expression of the *rut* operon is increased (31); and the UpBCon1 background, in which pyrimidines can be used as the sole nitrogen source at 37°C (see above). The UpBCon 1 strain (NCM4384) grows poorly at room temperature, and hence we generally studied its ability to catabolize pyrimidines at 37°C.

Strains carrying lesions in *rutA* or *-F* in any of the three backgrounds failed to grow on uridine as the sole nitrogen source (Table 5). Based on our *in vitro* results, this was expected for strains carrying lesions in *rutA* but not necessarily for strains carrying *rutF* lesions because RutF can be replaced *in vitro* by the flavin reductase Fre. Apparently no other flavin reductase can substitute for RutF *in vivo*. Whether this is because other flavin reductases are not present in sufficient amounts and/or do not have access to RutA or whether there is another explanation remains to be determined. In the *ntrB*-(Con) background, where levels of Rut enzymes are elevated, addition of uridine (5 mM) to the medium inhibited growth on ammonium (5 mM) at 37°C (doubling time increased from 2 to 3 h), indicating that a toxic intermediate(s) of the Rut pathway probably accumulated. Growth inhibition persisted in an *ntrB*-(Con) *rutF* strain (doubling time increased from 2 to 3 h). Uridine was not inhibitory in an *ntrB*(Con) *rutA* strain (doubling time remained 2 h in the presence of uridine), in agreement with the view that RutA is absolutely required to initiate uracil degradation. We obtained no suppressors of *rutA* in any background. However, we did obtain suppressors of *rutF* in the *ntrB*(Con) background. We showed that two such suppressors, which grew slowly on uridine and at different rates, released the usual 2 mol of nitrogen in utilizable form and that they excreted the usual 1 mol/mol of 3-hydroxypropionic acid into the medium (see Table S1 in the supplemental material) (31). Although we have not identified the suppressor lesions, their effects were as expected if they increased the amount or availability of another flavin reductase.

As was true of strains carrying *rutA* or *rutF* lesions, strains carrying a lesion in *rutB* in any of the three backgrounds we tested failed to grow on uridine as the sole nitrogen source (Table 5). As was the case for *rutA* strains, strains carrying a *rutB* lesion also failed to yield spontaneous suppressor mutations. In the *ntrB*(Con) background, where levels of Rut enzymes are elevated, addition of uridine to ammonium-containing medium markedly inhibited growth of the *rutB* strain at 37°C (data not shown), indicating that it probably accumulated a toxic intermediate(s). Based on what is known about the RutA/F and RutB reactions, this intermediate(s) would be ureidoacrylate and/or the peracid of ureidoacrylate (Fig. 5A and see the Discussion section).

Requirement for YdfG *in vivo*. We constructed strains carrying nonpolar deletions in *ydfG* in the three backgrounds described above. A strain with an insertion in *ydfG* in a wild-type background grew poorly on uridine as the sole nitrogen source, and an *ntrB*(Con) strain carrying the insertion did not grow at all (Table 5; see Fig. S4 in the supplemental material). The UpBCon1 strain carrying a *ydfG* insertion grew poorly on uridine at 37°C. Based on the fact that YdfG reduces malonic semialdehyde to 3-hydroxypropionic acid (see above) and therefore acts after both moles of NH_4^+ have been released from the pyrimidine ring, we infer that failure of strains

carrying *ydfG* insertions to grow well on uridine is due to toxicity of malonic semialdehyde *in vivo*.

Role of the RutG protein *in vivo*. In agreement with the bioinformatic prediction that the RutG protein was a nucleobase transporter (3, 32, 41), an otherwise wild-type strain carrying a *rutG* deletion failed to grow on the nucleobase uracil (0.5 mM or 2 mM) as the sole nitrogen source but used the nucleoside uridine normally. An *ntrB*(Con) *rutG* strain grew slowly on pyrimidine bases (uracil and thymine) and obtained both nitrogens from the ring. Residual growth may be accounted for by the fact that the *ntrB*(Con) lesion activates transcription of the gene(s) for other transporter(s) that can carry pyrimidine nucleosides/bases (59). Alternatively, or in addition, elevated expression of the *rut* operon in an *ntrB*(Con) strain may allow it to rely on a constitutively expressed transporter(s). An UpBCon1 *rutG* strain (NCM4384) grew well on pyrimidine bases at 37°C.

In the >20 occurrences of the *rut* operon outside the *Enterobacteriaceae*, *rutG* is retained only in *Acinetobacter* (see Table S2 in the supplemental material). Occasionally as in several methylobacteria, *rutG* is replaced by genes for a multisubunit transporter (ABC type) that appears to be a pyrimidine transporter and is, in other bacteria, associated with the operon for the reductive pathway of pyrimidine degradation (32, 38).

Requirement for the RutC to -E proteins *in vivo*. Although RutC was not required for release of ammonium *in vitro*, strains carrying *rutC* lesions in the wild-type or UpBCon1 background failed to grow on uridine as the nitrogen source (Table 5). This indicated that they probably accumulated a toxic intermediate that prevented their growth on the ammonium released from the pyrimidine ring. The *ntrB*(Con) *rutC* strain grew very slowly on uridine: it released both moles of nitrogen in utilizable form, but in contrast to its parental strain, released much less than 1 mol/mol of 3-hydroxypropionic acid into the medium (see Table S1 in the supplemental material). The latter finding indicated that RutC did not act on carbamate but probably acted on the 3-carbon intermediate released from the uracil ring (or on this portion of the molecule before hydrolysis by RutB). As explained in the Discussion, we speculate that toxicity is due to accumulation of the peracid of aminoacrylate. In the absence of RutC, cells apparently form less than the normal amount of malonic semialdehyde—and hence less 3-hydroxypropionic acid than usual—because a portion of the 3-carbon intermediate is diverted out of the Rut pathway. Although we obtained suppressors of *rutC* in the wild-type background, we did not identify them. Based on biochemical evidence, RutC was originally predicted to be an endoribonuclease (31, 36), but recently this has been questioned (32; see Discussion).

Like RutC, RutD was not required for release of ammonium *in vitro* but was required for growth on pyrimidines as the sole nitrogen source *in vivo* in the two backgrounds we tested (Table 5). The *rutD*::Kan insertion from which the original nonpolar *rutD* deletion was constructed may also have caused a decrease in RutC activity (see Materials and Methods) and was sufficiently toxic, even on enriched medium, that we inadvertently picked up suppressors when we introduced it into the wild-type and *ntrB*(Con) backgrounds. We studied one strain with a mutation that suppressed *rutD* in each background (NCM4088 and NCM4090, respectively). Both strains released the normal 2 mol of utilizable nitrogen from uridine but excreted much less than 1 mol/mol of 3-hydroxypropionic acid into the medium (see Table S1 in the supplemental material). This indicated that RutD, like RutC, did not act on carbamate but rather on the 3-carbon intermediate released from the uracil ring. The *rutD* suppressor strain NCM4088 excreted no detectable malonic acid into the growth medium (data not shown; examined as described by Loh et al. [31]), and NMR analysis of medium components failed to identify anything else excreted when it was grown on ^{13}C, ^{15}N-enriched uracil (data not shown). The *rutD* suppressor strain grew faster on uridine as the sole nitrogen source than its parental strain. Neither of the suppressor lesions was identified because we were not aware that they were present until we reconstructed a correct *rutD* deletion (*rutC*$^{+}$) in the wild-type and *ntrB*(Con) backgrounds late in the study (see Materials and Methods). As explained in the Discussion, we speculate that toxicity of a *rutD* deletion is due to the accumulation of aminoacrylate, even though it can hydrolyze spontaneously. As is the case for RutC, we think cells lacking RutD form less than the normal amount of malonic semialdehyde because a portion of the 3-carbon intermediate is diverted out of the Rut pathway.

Like RutC and RutD, RutE was required for growth on uridine *in vivo*, although it was not required for release of ammonium from pyrimidine rings *in vitro*. Wild-type or *ntrB*-(Con) strains with a nonpolar deletion in *rutE* failed to grow on uridine (Table 5; see Fig. S4 in the supplemental material). Addition of uridine to ammonium-containing medium inhibited growth of the *ntrB*(Con) *rutE* strain at 37°C, confirming that this strain probably accumulated a toxic intermediate. We obtained suppressors of *rutE* in the *ntrB*(Con) background but not in the wild-type background. The two that we studied released both moles of utilizable nitrogen from uridine and excreted 1 mol/mol of 3-hydroxypropionic acid into the medium (see Table S1 in the supplemental material). The latter distinguished them from the *ntrB*(Con) *rutC* strain and from suppressors of *rutD* and provided evidence that they formed a normal amount of malonic semialdehyde. As explained in the Discussion, we think that the function of RutE is the same as that of YdfG: i.e., reduction of malonic semialdehyde to 3-hydroxypropionic acid (see below for identification of the lesions in *rutE* suppressors and the logic for this argument).

Identification of *rutE* suppressors and lesions that allow growth on pyrimidines at 37°C. We obtained whole-genome sequence for strains carrying *rutE* suppressors or lesions that allowed growth on pyrimidines at 37°C and assembled and analyzed it as described in Materials and Methods. One of the *rutE* suppressors (NCM4299) had a frameshift lesion early in the *nemR* gene that should result in truncation of the NemR protein after 65 amino acids (Table 6). (Intact NemR is 171 amino acids.) The second *rutE* suppressor (NCM4300), which had the same growth rate on uridine as the first, had a lesion that disrupts the inverted repeat in the binding site for NemR/RutR in the promoter-regulatory region for the *nemRA* operon. Finally, the UpBCon2 strain (NCM4139), which was selected spontaneously to grow on pyrimidines at 37°C but which we studied very little, also had what appeared to be a damaging lesion in *nemR* that converted G141 to S. The UpBCon2 strain retains good ability to grow on pyrimidines at room temperature. Hence, we were able to introduce a nonpolar

TABLE 6. Identification of mutations that suppress Δ*rutE* and/or allow growth on uridine at 37°C

Strain	Phenotype	Type and site of mutation[a]	Effect of mutation
NCM4299	Suppression of Δ*rutE*	Single base change C1724300 deleted	*nemR* frameshift to NemR(1-65)
		Deletion of 11 kbp from 3924220 to 3935295	Deletion of all or part of *mioC*, *asnC*, *asnA*, *viaA*, *ravA*, *kup*, *rbsD*, *rbsA*, *rbsC*, and *rbsB*[b]
NCM4300	Suppression of Δ*rutE*	Single base change G1724029A	*nemR*; loss of dyad symmetry in NemR binding site[c]
		Deletion of 11 kbp from 3924220 to 3935295	Deletion of all or part of *mioC*, *asnC*, *asnA*, *viaA*, *ravA*, *kup*, *rbsD*, *rbsA*, *rbsC*, and *rbsB*[b]
NCM4139 (UpBcon2)	Growth on uridine at 37°C	Single base change G1724552A	NemR(G141S)
		lon::IS*186*	*lon* promoter disruption by IS insertion and duplication at 458014-458020
NCM4384 (UpBcon1)	Growth on uridine at 37°C	Single base change C3182707T	Alters structure of *sroG* riboswitch for *ribB*
		Deletion of 11 kbp from 3924220 to 3935295	Deletion of all or part of *mioC*, *asnC*, *asnA*, *viaA*, *ravA*, *kup*, *rbsD*, *rbsA*, *rbsC*, and *rbsB*[b]
		lon::IS*186*	*lon* promoter disruption by IS insertion and duplication at 458014-458020

[a] Genomic locations are given relative to *E. coli* K-12 strain MG1655 (NC_000913).

[b] This deletion was present in the Δ*rutE* strain from which suppressors were selected (NCM4115; Table 1) and was present in the *ntrB*(Con) *rutE*::Kan strain from which NCM4115 was constructed by FLPing. It was not present in the *ntrB*(Con) strain (NCM3876; Table 1) from which NCM4384 (UpBcon1) was selected spontaneously, and it was not present in NCM4103, NCM4101, or NCM4113.

[c] The NemR binding site (−13 to −28 relative to the sigma 70 promoter) for the *nemRA* operon is altered:

5′ TAGACCGACTGGTCTA 3′ to 5′ TAGACCGACTGATCTA 3′
3′ ATCTGGCTGACCAGAT 5′ 3′ ATCTGGCTGACTAGAT 5′.

rutE deletion into this strain and confirm that the NemR(G141S) lesion suppresses the loss of RutE at room temperature (Table 7; see Fig. S4 in the supplemental material). Likewise, we were able to introduce a nonpolar *nemR* deletion into the Δ*rutE* strain NCM4115 and show that it suppressed the loss of RutE at room temperature.

TABLE 7. Suppression of *rutE* and *ydfG* by increased expression of NemA or RibB

Strain	Relevant genotype[a]	Growth on uridine at:		Other lesion(s)
		Room temp	37°C	
NCM4115[b]	Δ*rutE*	−	−	*mioC*Δ
NCM4299[b]	Δ*rutE nemR*	+	−	*mioC*Δ
NCM4300[b]	Δ*rutE* p*nemR*[c]	+	−	*mioC*Δ
NCM4905[b]	Δ*rutE* Δ*nemR*	+	−	*mioC*Δ
NCM4906[d]	Δ*rutE nemR*	+	+/−[e]	*lon*
NCM4714	Δ*ydfG*	−	−	None
NCM4916[d]	Δ*ydfG nemR*	−[f]	+	*lon*
NCM4904[g]	Δ*nemR*	++	+	None
NCM4969[h]	*ydfG*::Kan Δ*nemR*	−[f]	+	None
NCM4509[i]	Δ*rutE sroG*	+	+/−	*mioC*Δ *lon*
NCM4715[i]	Δ*ydfG sroG*	−	+	*mioC*Δ *lon*

[a] All strains carry the same *ntrB*(Con) lesion. See Table 1 for construction and Table 6 for sequence changes.

[b] Congenic.

[c] Lesion in the promoter-regulatory region for *nemRA* that is predicted to prevent NemR repression (Table 6).

[d] Congenic with NCM4139 (UpBCon2).

[e] +/−, poor growth (see Fig. S4 in the supplemental material).

[f] Suppressors arise.

[g] Congenic with NCM3876.

[h] Congenic with NCM4904.

[i] Congenic with NCM4384 (UpBCon1).

The NemR protein is a repressor of *nemRA* transcription; relief of repression apparently requires alkylation of one or more of its cysteine residues (51). The NemA gene codes for the flavoprotein *N*-ethylmaleimide reductase, also referred to as the "old yellow enzyme" of *E. coli* (55). The fact that inactivation of NemR or inactivation of its binding site at *nemRA*—which would increase the amount of NemR—suppressed a *rutE* null lesion equally well (Table 7; see Fig. S4 in the supplemental material) indicates that suppression is likely to be due to increased expression of NemA, as does the finding that NemR apparently controls only *nemRA* transcription, despite the fact that *E. coli* contains very large amounts of it (51). Presumably, high levels of *N*-ethylmaleimide reductase can substitute for RutE. Although both of the *rutE* suppressors also carried a large deletion around *mioC*, which encodes a mysterious FMN binding protein (Table 6) (7), this deletion was not present in the UpBCon2 strain. We found that the *mioC* deletion had apparently been acquired when the *rutE*::Kan lesion was introduced into the *ntrB*(Con) background (but not the wild-type background) by phage P1-mediated transduction. Based on the results presented above, the *mioC* deletion is not central to *rutE* suppression. Using markers linked to *nemR* by phage P1-mediated transduction, we were able to show that the NemR(G141S) lesion in the UpBCon2 strain was both necessary and sufficient for growth on pyrimidines at 37°C in the *ntrB*(Con) background (K.-S. Kim and W. B. Inwood, unpublished observation). However, the robust growth of UpBCon2 also required a second mutation, which we identified as an insertion of IS*186* in the promoter region for the *lon* gene (Table 6). This insertion occurred in a hot spot and is known to eliminate Lon protease activity (42). We do not know its significance to our phenotype.

The UpBCon1 strain, which excreted a yellow compound that was identified as riboflavin (T. Mukherjee and T. Begley, personal communication), had a change in the riboswitch (called *sroG*) preceding the *ribB* (riboflavin B) gene (Table 6). The UpBCon1 strain had also acquired the deletion around *mioC* discussed above. Using markers linked to *ribB* by phage P1-mediated transduction, we showed that the *sroG* lesion was necessary and sufficient for growth on pyrimidines at 37°C (Kim and Inwood, unpublished). However, the robust growth of UpBCon1 also required the IS*186* insertion in the *lon* promoter described above. It did not require the deletion around *mioC*.

Changes in the riboswitch for the *rib* operon of *Bacillus subtilis* resulted in riboflavin excretion by increasing transcription of the operon (35, 56). Although the effects of changing the *ribB* riboswitch in *E. coli* are less clear, we presume that the lesion we have identified increases expression of *ribB* at either the transcriptional or translational level. Whether directly or indirectly, this appears to result in synthesis of excess riboflavin and its excretion, although the mechanism is not obvious.

Overlap in function of RutE and YdfG. To test whether inactivation of NemR, which suppressed a *rutE* deletion, also suppressed a *ydfG* lesion, we constructed a strain carrying both *nemR* and *ydfG* lesions as described in Materials and Methods. This strain, NCM4916 [NemR(G141S) *lon ntrB*(Con) Δ*ydfG*], grew faster on uridine at 37°C than a corresponding strain without the *nemR* mutation, NCM4714 [*ntrB*(Con) Δ*ydfG*] (Table 7; see Fig. S4 in the supplemental material), providing evidence that high levels of *N*-ethylmaleimide reductase can substitute for the short-chain dehydrogenase YdfG (18). Likewise, strain NCM4969 [Δ*nemR* Δ*ydfG ntrB*(Con)] grew faster than strain NCM4714, with which it was congenic. Thus, high levels of NemA can apparently substitute for either YdfG or RutE. (Suppression of *ydfG* was better at 37°C, and suppression of *rutE* was better at room temperature.) Suppression of both *rutE* and *ydfG* lesions by *nemR* lesions in turn links RutE to YdfG, whose function is known *in vitro*, and leads to the postulate mentioned above, namely, that RutE also reduces malonic semialdehyde to 3-hydroxypropionic acid.

The requirement for YdfG function or RutE function for utilization of uridine at 37°C was decreased in the UpBCon1 background (i.e., in the presence of the *sroG* lesion) (Table 7; see Fig. S4 in the supplemental material). This hints that large amounts of reduced flavin may also be able to drive reduction of malonic semialdehyde *in vivo*, either *per se* or through an unidentified enzyme(s).

DISCUSSION

In conjunction with a flavin reductase, RutA uses molecular oxygen to cleave the uracil ring between N-3 and C-4 (Fig. 5A and Fig. 6). NMR spectroscopic evidence that ^{18}O from O_2 was incorporated at C-4 (Fig. 3B) indicated that the product is not *N*-hydroxyureidoacrylate, as did evidence that N-3 was converted to NH_2 (see Fig. S2B in the supplemental material). The latter finding indicated that the product is not a 7-member ring compound in which oxygen is inserted between N-3 and C-4 (analogous to the Baeyer-Villiger rearrangement observed with cyclohexanone [40]), as did its mass (Fig. 4A). That ^{18}O was incorporated at C-4 indicated that the product was not obtained by hydrolysis of the 7-member ring compound to *N*-hydroxyureidoacrylate. The observed accurate masses of *m*/*z* 133.0491 and *m*/*z* 139.0565 (Fig. 4A) provided evidence for ureidoacrylate as the product. Finally, NMR spectroscopy indicated that the product obtained from the RutA/F (Fre) reaction *in vitro* is identical to chemically synthesized ureidoacrylate (Tables 2 and 3 and Fig. 5 and 6).

In both the reductive and oxidative pathways for pyrimidine catabolism described previously (22, 48, 52) the N-3–C-4 bond is cleaved hydrolytically after the C-5–C-6 double bond has been altered to decrease the aromaticity of the ring (Fig. 1). Although the product of the RutA/F reaction appears to result from hydrolytic cleavage at the same position, this is not consistent with the requirements for the reaction or with transfer of oxygen to C-4 from molecular O_2. Hence, we sought evidence for incorporation of both moles of oxygen from O_2 into the uracil ring. Mass spectrometry indicated the presence of a small amount of the peracid of ureidoacrylate in RutA reaction mixtures (Fig. 4B, 5, and 6). Work in a related article (37) shows that chemically synthesized ureidoacrylate peracid is rapidly reduced to ureidoacrylate under *in vitro* reaction conditions similar to ours (20 mM NADH rather than 4 mM and phosphate buffer at pH 8 rather than 7) and presents a plausible mechanism for the formation of ureidoacrylate peracid by RutA. This greatly strengthens the view that the peracid is the product of the RutA/F reaction and hence that RutA is an unusual oxygenase of a type not previously described (33, 34). We propose that it be called pyrimidine oxygenase.

The RutB protein, which has all the signatures of a cysteine hydrolase (32), hydrolyzes ureidoacrylate to yield 2 mol NH_3, CO_2, and malonic semialdehyde (Fig. 5B). Presumably, the initial products are carbamate and aminoacrylate, which are known to hydrolyze spontaneously. RutB is homologous to the ureidopropionase enzyme of the reductive pathway for pyrimidine ring degradation (39, 54), and its closest homologue is carbamoylsarcosine amidohydrolase (25, 32): both release CO_2 and NH_3 via carbamate. For reasons given below, we propose that RutB be called peroxyureidoacrylate/ureidoacrylate amido hydrolase.

There are several reasons we think the RutB protein hydrolyzes not only ureidoacrylate (Fig. 5B) but also its peracid (Fig. 6). First, the apparent half-life for reduction of the peracid *in vitro* is 5 min at 20 mM NADH at pH 8.0, and it is predicted to be at least this long *in vivo* because the concentrations of NADH and NADPH in *E. coli* are ≤0.2 mM each (2, 5, 20) and the total concentration of glutathione is on the order of 10 to 20 mM (5, 15). If reduction of the peracid *in vivo* is slow, some spontaneous decomposition—to ureidoacrylate, uracil, and undefined by-products (37)—could occur if RutB did not hydrolyze the peracid rapidly. Second, cell extracts of various *E. coli* strains yielded at most a trace of RutA/F product *in vitro* (Fig. 2A and B) (data for other strains not shown): rather, as radiolabeled uracil (C-2 or C-6) was consumed, the products of the RutB reaction appeared, indicating that hydrolysis by RutB was much faster than the RutA/F reaction. Third, as discussed below, RutC may catalyze reduction of aminoacrylate peracid, a product of the RutB reaction. Together, the evidence available indicates that ureidoacrylate peracid, the product of the RutA/F reaction, is probably the major substrate for RutB *in vivo* (Fig. 6), although clearly RutB can also

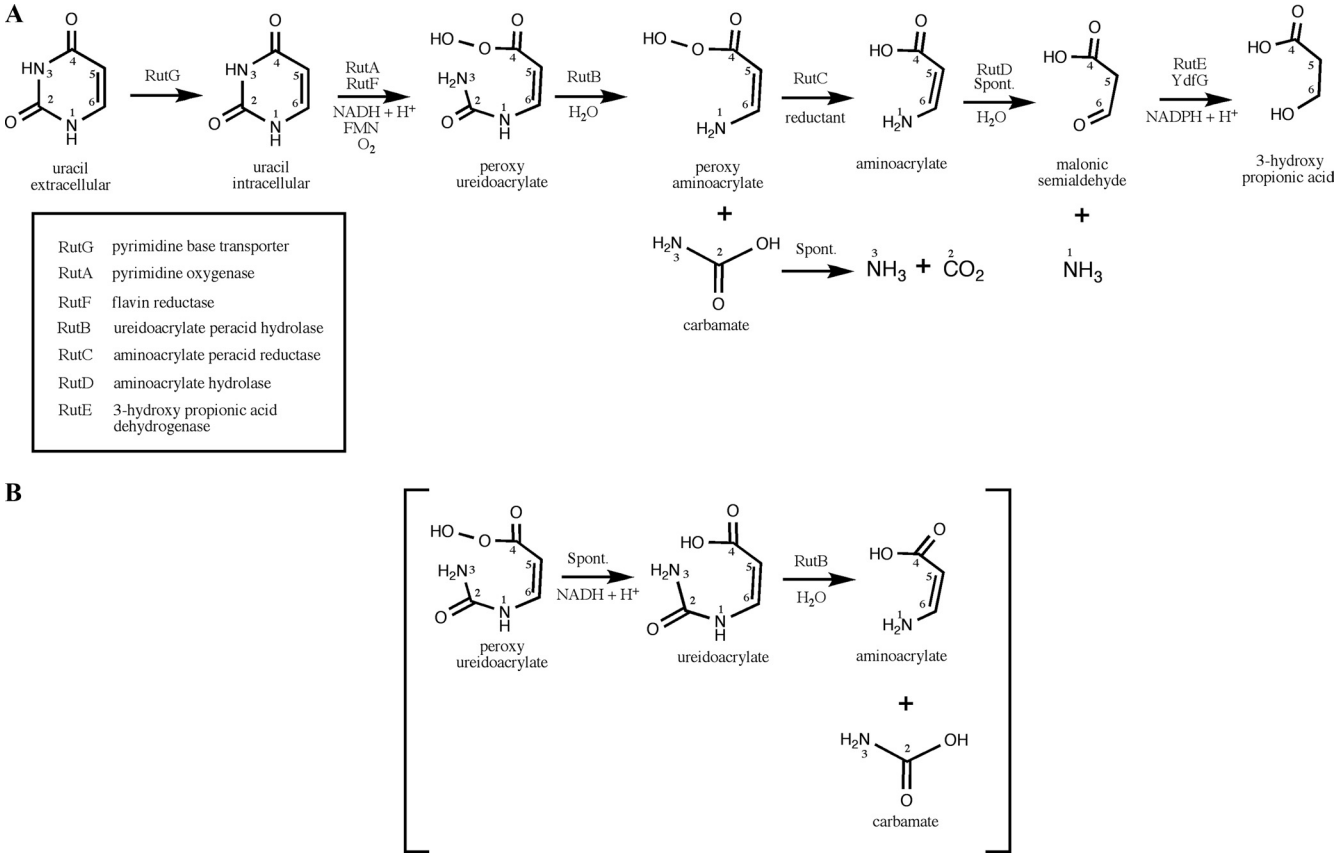

FIG. 6. Proposed *in vivo* pathway for pyrimidine ring degradation in *E. coli* K-12 (A) and possible handling of ureidoacrylate (B). (A) Rut pathway. RutG appears to be a pyrimidine nucleobase transporter. We infer that RutA catalyzes synthesis of ureidoacrylate peracid (see text). Although our work did not address the specific role of FMN, it is plausible that flavin hydroperoxide, a well-known intermediate in related reactions (40), would participate (37). We postulate that ureidoacrylate peracid is the primary substrate for RutB (see text). Activities of RutC, -D, and -E, which have not yet been studied biochemically, were inferred by a variety of other means. Whereas YdfG uses NADPH as a cofactor, RutE is predicted to be a flavoprotein (9, 27). Proposed names for Rut enzymes are in the inset. (B) Formation and use of ureidoacrylate. If some ureidoacrylate is formed by spontaneous reduction of ureidoacrylate peracid (37), RutB can hydrolyze it. We believe this auxiliary pathway, which was prominent *in vitro* (Fig. 5), plays a minor role *in vivo* (see text).

hydrolyze ureidoacrylate (Fig. 5B and Table 4; see Fig. S3 in the supplemental material).

In conjunction with RutA/F and RutB, the short-chain dehydrogenase YdfG (18) completes the Rut pathway *in vitro* by reducing malonic semialdehyde to 3-hydroxypropionic acid (Fig. 5C and 6). *In vivo* the absence of YdfG results in a growth defect or failure to grow on uridine as the sole nitrogen source in different genetic backgrounds, indicating that *E. coli* K-12 requires YdfG despite the fact that both moles of ammonium have already been released from the pyrimidine ring before it acts. Malonic semialdehyde appears to be toxic. Like other aldehydes, it can form adducts to free amino groups, and this may be the basis for its toxicity and the need to reduce it to the alcohol.

Evidence that RutE and YdfG have the same function. The RutE protein is predicted to belong to nitroreductase-like subfamily 5, which contains proteins of unknown function (9, 27, 32). Like members of the greater nitroreductase family, RutE is believed to use FMN as a cofactor. It is required for growth on uridine as the sole nitrogen source in both the wild-type and *ntrB*(Con) backgrounds (Table 7; see Fig. S4 in the supplemental material). Genetic evidence indicates that RutE has the same function as YdfG: i.e., both reduce malonic semialdehyde to 3-hydroxypropionic acid, although presumably by different mechanisms. Furthermore, the evidence indicates that toxicity of malonic semialdehyde, not the rate of release of ammonium, limits growth of *E. coli* K-12 on pyrimidines as the sole nitrogen source at high temperatures. The reasoning for these conclusions is as follows. First, relief of transcriptional repression of *nemA*, which codes for *N*-ethylmaleimide reductase, the "old yellow" enzyme of *E. coli*, suppresses the absence of either RutE or YdfG *in vivo* (Table 7; see Fig. S4 in the supplemental material). This would be expected if all three had the same biochemical function. In agreement with this view, overproduction of *N*-ethylmaleimide reductase in a *rutE* null strain results in excretion of the usual 1 mol/mol of 3-hydropropionic acid into the growth medium (see Table S1 in the supplemental material). Finally, overexpression of *N*-ethylmaleimide reductase allows an *ntrB*(Con) strain, which expresses the *rut* operon at high levels, to grow on pyrimidines as the sole nitrogen source at 37°C (although not as well as the UpBCon2 strain; see Results). Additional lines of bioinformatic evidence

support the view that RutE catalyzes reduction of malonic semialdehyde to 3-hydropropionate. First, the *rutE* gene is often absent from the *rut* operon (see Table S2 in the supplemental material), in agreement with the view that RutE acts after the nitrogens have been extracted from pyrimidine rings. Second, the five *rut* operons in *Acinetobacter* genomes (18 genomes total), all of which lack *rutE*, have a gene that codes for an enzyme in the same superfamily as YdfG and is predicted to reduce malonic semialdehyde and 2-methyl malonic semialdehyde to their corresponding alcohols (32). Finally, the *rut* operons in the two *Alteromonas* species for which whole genome sequences are available contain not only *rutE* but also the gene for an additional enzyme predicted to detoxify malonic semialdehyde by oxidizing it rather than reducing it (malonate semialdehyde/methyl malonate semialdehyde dehydrogenase, which would oxidize malonic semialdehyde to acetyl-*S*-coenzyme A [CoA]) (32, 50) (see Table S2 in the supplemental material). Neither genome carries a *ydfG* gene. Biochemical studies of RutE will be particularly interesting because flavoenzymes generally participate in oxidation of alcohols rather than reduction of aldehydes (24).

Speculations on RutD and RutC function. Like other Rut pathway proteins, both RutD and RutC are required for growth on uridine as the sole nitrogen source, despite the fact that they are not required for release of ammonium *in vitro*. We speculate that RutD, a hypothetical α/β-hydrolase with no close relatives (32), increases the rate of spontaneous hydrolysis of aminoacrylate to malonic semialdehyde (Fig. 6). This would be analogous to the role of carbonic anhydrases in accelerating the rate of spontaneous hydration of CO_2.

Finally, we speculate that RutC, a member of a family of proteins without a clearly defined function (32), reduces the peracid of aminoacrylate to aminoacrylate, the substrate for RutD (Fig. 6). Members of the RutC family appear to bind toxic metabolic intermediates (10, 14). Both of the other members of the family in *E. coli*, TdcF (*t*hreonine *d*eaminase *c*atabolic *F*) and YjgF, appear to be involved in metabolism of the toxic intermediate 2-ketobutyrate (8, 10, 14, 29). Structurally, RutC family proteins are trimers with binding clefts for small ligands at monomer interfaces (53). In the clefts, they carry an invariant R that is often followed by XC. The structure of the *E. coli* TdcF protein has been determined with 2-ketobutyrate bound: oddly, it was bound as the rare enol tautomer, with its carboxylate group doubly hydrogen bonded to the guanidinium group of the invariant R and its enol OH group bonded to both the backbone amide of the conserved C and the carboxyl group of the conserved E120 in the adjacent subunit (8) (see Fig. S5 in the supplemental material). The side chain of the corresponding C in the *E. coli* YjgF protein—whose structure has been determined only in its unliganded form—was derivatized with what appeared to be a thiophosphate or a thiosulfate (53). By analogy to what is known about TdcF and YjgF, we postulate that RutC binds the peracid form of aminoacrylate (see Fig. S5 in the supplemental material) and that it may use the $XC^{107}XXC^{110}$ motif adjacent to its invariant R^{105} to reduce the peracid to the carboxylic acid (aminoacrylate). If RutC binds aminoacrylate peracid in its stable amine form—as would be predicted—it would also inhibit spontaneous hydrolysis of the amino group. When aminoacrylate was released by RutC, RutD could then increase its spontaneous rate of hydrolysis by catalyzing formation of the rare imine tautomer. The roles of RutC and RutD would be to insure that reduction of the peracid form of aminoacrylate and hydrolysis of aminoacrylate occur rapidly and in a particular order. These admittedly speculative ideas provide a framework for further biochemical and genetic studies. In the latter connection, it will be interesting to determine the identities of *rutC* and *rutD* suppressors, for which tools are now available (see Materials and Methods), and to understand why a *rutC* strain and *rutD* suppressors go off the pathway and excrete less than the usual amount of 3-hydroxypropionic acid into the medium (see Table S1 in the supplemental material). Apparently, they generate less than the usual amount of toxic malonic semialdehyde (see Results).

Conclusions. In summary, Rut pathway enzymes oxidatively cleave the pyrimidine ring to produce a series of reactive, toxic intermediates that includes strong oxidizing agents (peracids) and compounds known to polymerize readily (ureidoacrylates and aminoacrylates) or form adducts (malonic semialdehyde) (Fig. 6). Only half of the Rut enzymes (RutA, RutF, and RutB) are required *in vitro* to release both nitrogens from the pyrimidine ring as NH_4^+ (Fig. 5). The other half (RutC, RutD, and RutE) are nonetheless required *in vivo*, apparently to prevent accumulation of toxic intermediates and by-products. We postulate that they act in order on the 3-carbon intermediate released by RutB (Fig. 6). The function of RutE overlaps with that of the short-chain dehydrogenase YdfG (Tables 6 and 7; see Fig. S4 in the supplemental material), and both are required *in vivo*: apparently neither alone has sufficient activity, and the two together are still not sufficient for growth at 37°C.

Although *E. coli* does not grow on pyrimidines as the sole nitrogen source at 37°C, it transcribes the *rut* operon very highly at this temperature under nitrogen-limiting conditions (31, 59). Presumably the Rut pathway allows *E. coli* to use pyrimidines, which are readily available degradation products of RNA, as part of the nitrogen source at 37°C. (The YdfG protein, which is coded for outside the *rut* operon, may not be required under these circumstances.) Forcing their use as the sole nitrogen source at any temperature is a trick of the experimentalist. The *rut* operon is highly expressed, even in the absence of exogenous pyrimidines. Whether the Rut pathway is also used to decrease the internal free pool concentrations of pyrimidines under nitrogen-limiting conditions and/or to generate toxic intermediates that help slow the growth of *E. coli* in a coordinated way are intriguing possibilities that remain to be explored.

ACKNOWLEDGMENTS

We thank the National BioResource Project of the National Institute of Genetics, Japan, for *E. coli* Keio strains and ASKA strains. We thank Michael Coyle for initiating studies of RutG and for attempting to determine the fate of carbons 4 to 6 of uracil in a *rutD* suppressor strain, Rebecca Fong for help with strain construction, and Zhongrui Zhou for 3-hydroxypropionic acid determinations. We thank Hans Liao for the gift of 3-hydroxypropionic acid and for alerting us to the possible role of the YdfG protein in its formation, and we thank Chris Walsh for alerting us to a mechanism by which RutD could increase the rate of aminoacrylate hydrolysis. We are grateful to Luying Xun, Washington State University, for gifts of purified Fre enzyme and a strain that overexpresses Fre and for continued interest in the work. Finally, we are indebted to Tadhg Begley for suggesting that the small amount of RutA product with a mass indicating that both atoms of O_2 had been incorporated might be ureidoacrylate peracid.

This work was supported by NIH grant GM38361 to S.K. The Central California 900-MHz facility was supported by NIH grant

GM68933. We thank the NSF (BBS 01-19304) and NIH (RR15756) for funding for the 800-MHz NMR and BBS 87-20134 for funding for the 600-MHz NMR.

REFERENCES

1. **Andersen, G., O. Björnberg, S. Polakova, Y. Pynyaha, A. Rasmussen, K. Møller, A. Hofer, T. Moritz, M. P. Sandrini, A. M. Merico, C. Compagno, H. E. Akerlund, Z. Gojković, and J. Piskur.** 2008. A second pathway to degrade pyrimidine nucleic acid precursors in eukaryotes. J. Mol. Biol. **380:** 655–666.
2. **Andersen, K. B., and K. von Meyenburg.** 1977. Charges of nicotinamide adenine nucleotides and adenylate energy charge as regulatory parameters of the metabolism in *Escherichia coli*. J. Biol. Chem. **252:**4151–4156.
3. **Andersen, P. S., D. Frees, R. Fast, and B. Mygind.** 1995. Uracil uptake in *Escherichia coli* K-12: isolation of *uraA* mutants and cloning of the gene. J. Bacteriol. **177:**2008–2012.
4. **Baba, T., T. Ara, M. Hasegawa, Y. Takai, Y. Okumura, M. Baba, K. A. Datsenko, M. Tomita, B. L. Wanner, and H. Mori.** 2006. Construction of *Escherichia coli* K-12 in-frame, single-gene knockout mutants: the Keio collection. Mol. Syst. Biol. **2:**2006.0008.
5. **Bennett, B. D., E. H. Kimball, M. Gao, R. Osterhout, S. J. Van Dien, and J. D. Rabinowitz.** 2009. Absolute metabolite concentrations and implied enzyme active site occupancy in *Escherichia coli*. Nat. Chem. Biol. **5:**593–599.
6. **Bertini, I., I. C. Felli, L. Gonnelli, R. Pierattelli, Z. Spyranti, and G. A. Spyroulias.** 2006. Mapping protein-protein interaction by $^{13}C'$-detected heteronuclear NMR spectroscopy. J. Biomol. NMR **36:**111–122.
7. **Birch, O. M., K. S. Hewitson, M. Fuhrmann, K. Burgdorf, J. E. Baldwin, P. L. Roach, and N. M. Shaw.** 2000. MioC is an FMN-binding protein that is essential for *Escherichia coli* biotin synthase activity *in vitro*. J. Biol. Chem. **275:**32277–32280.
8. **Burman, J. D., C. E. Stevenson, R. G. Sawers, and D. M. Lawson.** 2007. The crystal structure of Escherichia coli TdcF, a member of the highly conserved YjgF/YER057c/UK114 family. BMC Struct. Biol. **7:**30.
9. **Choi, J. W., J. Lee, K. Nishi, Y. S. Kim, C. H. Jung, and J. S. Kim.** 2008. Crystal structure of a minimal nitroreductase, ydjA, from *Escherichia coli* K12 with and without FMN cofactor. J. Mol. Biol. **377:**258–267.
10. **Christopherson, M. R., G. E. Schmitz, and D. M. Downs.** 2008. YjgF is required for isoleucine biosynthesis when *Salmonella enterica* is grown on pyruvate medium. J. Bacteriol. **190:**3057–3062.
11. **Datsenko, K. A., and B. L. Wanner.** 2000. One-step inactivation of chromosomal genes in *Escherichia coli* K-12 using PCR products. Proc. Natl. Acad. Sci. U. S. A. **97:**6640–6645.
12. **Delaglio, F., S. Grzesiek, G. W. Vuister, G. Zhu, J. Pfeifer, and A. Bax.** 1995. NMRPipe: a multidimensional spectral processing system based on UNIX pipes. J. Biomol. NMR **6:**277–293.
13. **Eichhorn, E., J. R. van der Ploeg, and T. Leisinger.** 1999. Characterization of a two-component alkanesulfonate monooxygenase from *Escherichia coli*. J. Biol. Chem. **274:**26639–26646.
14. **Enos-Berlage, J. L., M. J. Langendorf, and D. M. Downs.** 1998. Complex metabolic phenotypes caused by a mutation in *yjgF*, encoding a member of the highly conserved YER057c/YjgF family of proteins. J. Bacteriol. **180:** 6519–6528.
15. **Fahey, R. C., W. C. Brown, W. B. Adams, and M. B. Worsham.** 1978. Occurrence of glutathione in bacteria. J. Bacteriol. **133:**1126–1129.
16. **Farkas, J., J. Hapala, O. Jindrova, and J. Skoda.** 1982. Reaction of 2,3-dihydro-1,3-6H-oxazine-2,6-dione with aliphatic amines and amino acids Collect. Czech Chem. Commun. (Camb.) **47:**2932–2945.
17. **Fox, C. H., F. B. Johnson, J. Whiting, and P. P. Roller.** 1985. Formaldehyde fixation. J. Histochem. Cytochem. **33:**845–853.
18. **Fujisawa, H., S. Nagata, and H. Misono.** 2003. Characterization of short-chain dehydrogenase/reductase homologues of *Escherichia coli* (YdfG) and *Saccharomyces cerevisiae* (YMR226C). Biochim. Biophys. Acta **1645:**89–94.
19. **Galán, B., E. Díaz, M. A. Prieto, and J. García.** 2000. Functional analysis of the small component of the 4-hydroxyphenylacetate 3-monooxygenase of *Escherichia coli* W: a prototype of a new flavin:NAD(P)H reductase subfamily. J. Bacteriol. **182:**627–636.
20. **Grose, J. H., L. Joss, S. F. Velick, and J. R. Roth.** 2006. Evidence that feedback inhibition of NAD kinase controls responses to oxidative stress. Proc. Natl. Acad. Sci. U. S. A. **103:**7601–7606.
21. **Gyaneshwar, P., O. Paliy, J. McAuliffe, D. L. Popham, M. I. Jordan, and S. Kustu.** 2005. Sulfur and nitrogen limitation in *Escherichia coli* K-12: specific homeostatic responses. J. Bacteriol. **187:**1074–1090.
22. **Hayaishi, O., and A. Kornberg.** 1952. Metabolism of cytosine, thymine, uracil, and barbituric acid by bacterial enzymes. J. Biol. Chem. **197:**717–732.
23. **Inwood, W. B., J. A. Hall, K.-S. Kim, L. Demirkhanyan, D. Wemmer, H. Zgurskaya, and S. Kustu.** 2009. Epistatic effects of the protease/chaperone HflB on some damaged forms of the *Escherichia coli* ammonium channel AmtB. Genetics **183:**1327–1340.
24. **Kalliri, E., S. B. Mulrooney, and R. P. Hausinger.** 2008. Identification of *Escherichia coli* YgaF as an L-2-hydroxyglutarate oxidase. J. Bacteriol. **190:** 3793–3798.
25. **Kim, J. M., S. Shimizu, and H. Yamada.** 1986. Purification and characterization of a novel enzyme, N-carbamoylsarcosine amidohydrolase, from *Pseudomonas putida* 77. J. Biol. Chem. **261:**11832–11839.
26. **Kitagawa, M., T. Ara, M. Arifuzzaman, T. Ioka-Nakamichi, E. Inamoto, H. Toyonaga, and H. Mori.** 2005. Complete set of ORF clones of *Escherichia coli* ASKA library (a complete set of E. coli K-12 ORF archive): unique resources for biological research. DNA Res. **12:**291–299.
27. **Koike, H., H. Sasaki, T. Kobori, S. Zenno, K. Saigo, M. E. Murphy, E. T. Adman, and M. Tanokura.** 1998. 1.8 Å crystal structure of the major NAD(P)H:FMN oxidoreductase of a bioluminescent bacterium, Vibrio fischeri: overall structure, cofactor and substrate-analog binding, and comparison with related flavoproteins. J. Mol. Biol. **280:**259–273.
28. **Kornberg, A.** 2006. Osamu Hayaishi: pioneer first of the oxygenases, then the molecular basis of sleep and throughout a great statesman of science. IUBMB Life **58:**253.
29. **LaRossa, R. A., and T. K. Van Dyk.** 1987. Metabolic mayhem caused by 2-ketoacid imbalances. Bioessays **7:**125–130.
30. **Liu, X., and R. E. Parales.** 2008. Chemotaxis of *Escherichia coli* to pyrimidines: a new role for the signal transducer Tap. J. Bacteriol. **190:**972–979.
31. **Loh, K. D., P. Gyaneshwar, E. Markenscoff Papadimitriou, R. Fong, K.-S. Kim, R. Parales, Z. Zhou, W. Inwood, and S. Kustu.** 2006. A previously undescribed pathway for pyrimidine catabolism. Proc. Natl. Acad. Sci. U. S. A. **103:**5114–5119.
32. **Marchler-Bauer, A., J. B. Anderson, F. Chitsaz, M. K. Derbyshire, C. DeWeese-Scott, J. H. Fong, L. Y. Geer, R. C. Geer, N. R. Gonzales, M. Gwadz, S. He, D. I. Hurwitz, J. D. Jackson, Z. Ke, C. J. Lanczycki, C. A. Liebert, C. Liu, F. Lu, S. Lu, G. H. Marchler, M. Mullokandov, J. S. Song, A. Tasneem, N. Thanki, R. A. Yamashita, D. Zhang, N. Zhang, and S. H. Bryant.** 2009. CDD: specific functional annotation with the Conserved Domain Database. Nucleic Acids Res. **37:**D205–D210.
33. **Massey, V.** 1994. Activation of molecular oxygen by flavins and flavoproteins. J. Biol. Chem. **269:**22459–22462.
34. **Massey, V.** 2000. The chemical and biological versatility of riboflavin. Biochem. Soc. Trans. **28:**283–296.
35. **Mironov, A. S., I. Gusarov, R. Rafikov, L. E. Lopez, K. Shatalin, R. A. Kreneva, D. A. Perumov, and E. Nudler.** 2002. Sensing small molecules by nascent RNA: a mechanism to control transcription in bacteria. Cell **111:** 747–756.
36. **Morishita, R., A. Kawagoshi, T. Sawasaki, K. Madin, T. Ogasawara, T. Oka, and Y. Endo.** 1999. Ribonuclease activity of rat liver perchloric acid-soluble protein, a potent inhibitor of protein synthesis. J. Biol. Chem. **274:**20688–20692.
37. **Mukherjee, T., Y. Zhang, S. Abdelwahed, S. Ealick, and T. Begley.** 2010. Catalysis of flavoenzyme-mediated amide hydrolysis. J. Am. Chem. Soc. **132:**5550–5551.
38. **Osterman, A.** 2006. A hidden metabolic pathway exposed. Proc. Natl. Acad. Sci. U. S. A. **103:**5637–5638.
39. **Romão, M. J., D. Turk, F. X. Gomis-Rüth, R. Huber, G. Schumacher, H. Möllering, and L. Rüssmann.** 1992. Crystal structure analysis, refinement and enzymatic reaction mechanism of N-carbamoylsarcosine amidohydrolase from *Arthrobacter* sp. at 2.0 A resolution. J. Mol. Biol. **226:**1111–1130.
40. **Ryerson, C. C., D. P. Ballou, and C. Walsh.** 1982. Mechanistic studies on cyclohexanone oxygenase. Biochemistry **21:**2644–2655.
41. **Saier, M. H., Jr., B. H. Eng, S. Fard, J. Garg, D. A. Haggerty, W. J. Hutchinson, D. L. Jack, E. C. Lai, H. J. Liu, D. P. Nusinew, A. M. Omar, S. S. Pao, I. T. Paulsen, J. A. Quan, M. Sliwinski, T. T. Tseng, S. Wachi, and G. B. Young.** 1999. Phylogenetic characterization of novel transport protein families revealed by genome analyses. Biochim. Biophys. Acta **1422:**1–56.
42. **SaiSree, L., M. Reddy, and J. Gowrishankar.** 2001. IS*186* insertion at a hot spot in the lon promoter as a basis for lon protease deficiency of *Escherichia coli* B: identification of a consensus target sequence for IS*186* transposition. J. Bacteriol. **183:**6943–6946.
43. **Schleucher, J., M. Schwendinger, M. Sattler, P. Schmidt, O. Schedletzky, S. Glaser, O. W. Sørensen, and C. Griesinger.** 1994. A general enhancement scheme in heteronuclear multidimensional NMR employing pulsed field gradients. J. Biomol. NMR **4:**301–306.
44. **Shimada, T., K. Hirao, A. Kori, K. Yamamoto, and A. Ishihama.** 2007. RutR is the uracil/thymine-sensing master regulator of a set of genes for synthesis and degradation of pyrimidines. Mol. Microbiol. **66:**744–757.
45. **Shimada, T., A. Ishihama, S. J. Busby, and D. C. Grainger.** 2008. The *Escherichia coli* RutR transcription factor binds at targets within genes as well as intergenic regions. Nucleic Acids Res. **36:**3950–3955.
46. **Simaga, S., and E. Kos.** 1978. Uracil catabolism by *Escherichia coli* K12S. Z. Naturforsch. C **33:**1006–1008.
47. **Simaga, S., and E. Kos.** 1981. Properties and regulation of pyrimidine catabolism in *Escherichia coli*. Int. J. Biochem. **13:**615–619.
48. **Soong, C. L., J. Ogawa, E. Sakuradani, and S. Shimizu.** 2002. Barbiturase, a novel zinc-containing amidohydrolase involved in oxidative pyrimidine metabolism. J. Biol. Chem. **277:**7051–7058.
49. **Soupene, E., W. C. van Heeswijk, J. Plumbridge, V. Stewart, D. Bertenthal, H. Lee, G. Prasad, O. Paliy, P. Charernnoppakul, and S. Kustu.** 2003. Physiological studies of *Escherichia coli* strain MG1655: growth defects and apparent cross-regulation of gene expression. J. Bacteriol. **185:**5611–5626.

50. **Stines-Chaumeil, C., F. Talfournier, and G. Branlant.** 2006. Mechanistic characterization of the MSDH (methylmalonate semialdehyde dehydrogenase) from *Bacillus subtilis*. Biochem. J. **395:**107–115.
51. **Umezawa, Y., T. Shimada, A. Kori, K. Yamada, and A. Ishihama.** 2008. The uncharacterized transcription factor YdhM is the regulator of the *nemA* gene, encoding *N*-ethylmaleimide reductase. J. Bacteriol. **190:**5890–5897.
52. **Vogels, G. D., and C. Van der Drift.** 1976. Degradation of purines and pyrimidines by microorganisms. Bacteriol. Rev. **40:**403–468.
53. **Volz, K.** 1999. A test case for structure-based functional assignment: the 1.2 A crystal structure of the *yjgF* gene product from *Escherichia coli*. Protein Sci. **8:**2428–2437.
54. **Walsh, T. A., S. B. Green, I. M. Larrinua, and P. R. Schmitzer.** 2001. Characterization of plant beta-ureidopropionase and functional overexpression in *Escherichia coli*. Plant Physiol. **125:**1001–1011.
55. **Williams, R. E., and N. C. Bruce.** 2002. 'New uses for an Old Enzyme'—the Old Yellow Enzyme family of flavoenzymes. Microbiology **148:**1607–1614.
56. **Winkler, W. C., S. Cohen-Chalamish, and R. R. Breaker.** 2002. An mRNA structure that controls gene expression by binding FMN. Proc. Natl. Acad. Sci. U. S. A. **99:**15908–15913.
57. **Wishart, D. S., C. G. Bigam, J. Yao, F. Abildgaard, H. J. Dyson, E. Oldfield, J. L. Markley, and B. D. Sykes.** 1995. ^{1}H, ^{13}C and ^{15}N chemical shift referencing in biomolecular NMR. J. Biomol. NMR **6:**135–140.
58. **Xun, L., and E. R. Sandvik.** 2000. Characterization of 4-hydroxyphenylacetate 3-hydroxylase (HpaB) of *Escherichia coli* as a reduced flavin adenine dinucleotide-utilizing monooxygenase. Appl. Environ. Microbiol. **66:**481–486.
59. **Zimmer, D. P., E. Soupene, H. L. Lee, V. F. Wendisch, A. B. Khodursky, B. J. Peter, R. A. Bender, and S. Kustu.** 2000. Nitrogen regulatory protein C-controlled genes of *Escherichia coli*: scavenging as a defense against nitrogen limitation. Proc. Natl. Acad. Sci. U. S. A. **97:**14674–14679.